Activation of AMP-activated protein kinase signaling pathway ameliorates steatosis in laying hen hepatocytes

Kun Zhang,[*,1] Yan Shi,[†,1] Chunli Huang,[*] Cheng Huang,[*] Puzhi Xu,[*] Changming Zhou,[*] Ping Liu,[*] Ruiming Hu,[*] Yu Zhuang,[*] Guyue Li,[*] Guoliang Hu,[*] and Xiaoquan Guo[*,2]

Jiangxi Provincial Key Laboratory for Animal Health, College of Animal Science and Technology, Jiangxi Agricultural University, Nanchang, Jiangxi, China; and †School of Computer and Information Engineering, Jiangxi Agricultural University, Nanchang, Jiangxi, China

ABSTRACT The fatty liver hemorrhage syndrome in laying hens is a disease of lipid metabolism disorders. Importantly, energy sensor AMP-activated protein kinase (AMPK) plays an essential role in homeostasis regulation of liver lipid. The current research aims to investigate the relationship between AMPK signaling pathway and lipid metabolism in laying hen hepatocytes and explore the underlying mechanisms. The steatotic hepatocytes model of laying hen was established and treated with AMPK agonist AICAR and inhibitor compound C. The results showed that the levels of triglyceride, total cholesterol, and low-density lipoprotein cholesterol significantly declined while high-density lipoprotein cholesterol level increased in the AICAR-treated steatosis group compared with the steatosis group. Furthermore, the mRNA levels of liver kinase B1 and AMP-activated protein kinase α1 declined significantly in the steatosis group compared with those in the normal group. However, AMPK activation significantly upregulated the mRNA levels of peroxisome proliferator-activated receptor α and carnitine palmitoyl transferase-1 while downregulated the mRNA levels of acetyl CoA carboxylase, fatty acid synthase, 3-hydroxy-3-methyl glutaryl coenzyme A reductase, Sn-glycerol-3-phosphate acyltransferase, and hepatocyte nuclear factor 4α. These results suggest that activated AMPK signaling pathway increases fatty acid oxidation and reduces lipid synthesis in laying hen hepatocytes, thereby ameliorating liver steatosis.

Key words: FLHS, AMPK signaling pathway, lipid metabolism, laying hen, hepatocyte

INTRODUCTION

Fatty liver hemorrhage syndrome (FLHS) in laying hens, a disorder of lipid metabolism, is characterized by steatosis and different degrees of bleeding in the liver. It was first reported in 1956. Importantly, FLHS mostly occurs in caged layer hens during the peak period of egg production, with the sharp drop in egg production and the sudden death of chickens in good condition being the main manifestations. According to reports, 74% of the total mortality of caged laying hens is caused by FLHS in Queensland, Australia (Rozenboim et al., 2016). Moreover, in northern California, FLHS is the most common noncommunicable cause of death (Mete et al., 2013). At present, FLHS has become a common chicken disease in many countries. With the rapid development of the poultry industry, the incidence of FLHS is increasing year by year, which has brought huge losses to the poultry industry. Nutrition, environment, hormones, and genetic factors are considered to be possible causes of FLHS (Gao et al., 2019). Among them, nutritional factors are regarded as the main reason. However, so far, the exact pathogenesis of FLHS is not completely clear. Related research still needs to be carried out in large quantities.

The energy sensor AMP-activated protein kinase (AMPK) plays a significant role in the homeostasis regulation of liver lipid. Because of its characteristics in regulating various pathways of metabolism, including lipid metabolism of liver, it has attracted extensive attentions. Previous studies have showed that activation of AMPK stimulates the oxidation of fatty acids (FA) and reduces the synthesis of cholesterol and triglycerides in the liver of mammals (Winder and Hardie, 1999).

Furthermore, study showed that activated AMPK can restrain the formation of *de novo* lipid and prevent the development of fatty liver (Cheng et al., 2018). Overexpression of sterol regulatory element binding protein 1c (SREBP 1c) will lead to increased generation of *de novo* fat in liver, while the activation of AMPK with small molecule activators can significantly reduce liver lipids (Boudaba et al., 2018). These studies suggested that activated AMPK signaling pathway may cause dramatic changes of lipid metabolism in liver cells, emphasizing the powerful effect of AMPK activation on fatty liver therapy. This included increased oxidation of liver fat and reduced synthesis of liver triglyceride and cholesterol. In view of its multiple functions on lipid metabolism, the reduction or loss of AMPK activity has been conceived as a critical pathogenic factor in the developmental process of the metabolic disorders as well as fatty liver (Ruderman et al., 2013). This assumption is supported by the phenomena that multiple animals with fatty liver have reduced AMPK activity in the liver (Muse et al., 2004).

The increasing studies indicated that AMPK signaling pathway plays an indispensable role in ameliorating liver lipid metabolism. However, regrettably, the current research on the relationship between AMPK signaling pathway and fatty liver is mainly focused on humans and mice, while it is extremely rare in chickens, especially in laying hens. Therefore, at present, little is known about the relationship between AMPK signaling pathway and fatty liver as well as fatty degeneration in laying hens. To further investigate the contribution of AMPK signaling pathway in lipid metabolism in layer liver cells and to explore its underlying mechanisms of action, we used the layer primary hepatocytes cultured *in vitro* as the biological model to conduct experiments. This study may provide new strategies for the treatment and prevention of FLHS in laying hens. In addition, to some extent, it may also provide hints for further research on nonalcoholic fatty liver disease in humans.

MATERIALS AND METHODS

Experimental Animal and Management

In this experiment, 180-day-old adult Hy-Line Brown layers were bought from Guohua Poultry Breeding Co., Ltd., Nanchang 330000, China. All layers adapted for 4 wk, during which a basic diet was provided. Besides, all of them were free to eat and drink and gave enough light in experimental period. Exhaust fan, warm lights, and hanging thermometer were installed in the test animal house, and the room temperature ($18°C–23°C$) and lighting (16 h) were controlled in accordance with the commercial conditions. Standard formula feed was purchased from Zhengda feed mill in Nanchang 330000, China. Before the experiment, all laying hens were anesthetized with pentobarbital sodium and then sacrificed by bloodletting. The present study was approved by the College of Animal Science and Technology, Jiangxi Agricultural University, and all the experimental

procedures were performed according to the institutional guidelines of animal care and use committee.

Isolation and Culture of Primary Liver Cells in Laying Hens

The primary liver cells of laying hens were isolated by using the method of modified situ 2-step perfusion according to a previous study (Li et al., 2019), and then the cell survival rate was detected by Trypan Blue staining. When the cell survival rate confirmed by Trypan Blue staining reached 90 to 95%, viable liver cells at the density of 10^5 to 10^6 cells/mL were seeded in 6-well plates and cultured in the complete medium (Dulbecco's modified Eagle's medium) containing 10% fetal bovine serum, 1% double-resistance penicillin-streptomycin solution, 10^{-7} mol/L dexamethasone, 6.25 ng/mL transferrin, and 10 μg/mL vitamin C at $37°C$ in a humidified atmosphere of 5% CO_2. The medium was changed every 12 h.

After 2 d, when the liver cells reached the enough confluence, the medium was removed, and the liver cells were maintained in serum-free medium for 24 h. Then, the cultures were obtained, and the activity of liver cells was determined by cck8 assay.

Establishment and Identification of Steatosis Liver Cells Model

In order to induce FA overloading, liver cells at 70% confluence were exposed to a mixture of FA (containing oleic acid, palmitic acid in proportions of 2:1). The liver cells were collected for identification after modeling 1.5 h, 6 h, 12 h, and 24 h. To measure the accumulation of neutral lipid droplet, the cells were stained by the Oil Red O method.

After treatment by FA, the cells were washed with iced phosphate-buffered saline (PBS) for 2 times and fixed with 10% paraformaldehyde for 1 h. After fixation, the cells were washed with PBS again and stained with freshly prepared Oil Red O solution for 30 min at room temperature. Then, the cells were rinsed with distilled water to clear away unbound dye, and the hematoxylin was used to counterstain the hepatocyte nuclei. After staining, the distribution and state of lipid droplets were observed with a microscope and pictures were taken. Besides, to quantitate the Oil Red O content, isopropanol was added to each sample and shaked for 5 min to extract the dye. In the end, we read the samples by spectrophotometry at 490 nm.

Determination of the Effective Duration of Activation and Inhibition of AICAR and Compound C in Primary Liver Cells

The liver cells were collected with a cell scraper and inoculated in a 6-well plate by 2 mL per hole with a concentration of $1 × 10^6$ cell/mL. We prepared complete medium containing 0.5 mmol/L AICAR and 20 μmol/L

compound C to cultivate the liver cells. Then, the AMPK activity in the specimens was determinated by double-antibody sandwich ELISA method with a microplate reader at 0.5 h, 1.5 h, 6 h, 12 h, 24 h, and 48 h. Every time, the liver cells were collected into a centrifuge tube and washed with cold PBS for 2 times, and the cells were lysed in lysis buffer and centrifuged to obtain the supernatant for determination of the AMPK activity. In the end, the AMPK activity curve was plotted.

After the aforementioned series of work, the experiment was divided into the following 4 groups: normal hepatocytes (NH) group, steatosis hepatocytes (SH) group, SH + AICAR group, and SH + compound C group.

According to the effective duration of activation and inhibition of AICAR and compound C in primary liver cells, we respectively collected the liver cells after 1.5 h and 24 h of treatment. First of all, the liver cells were washed with PBS buffer solution and then scraped down by cell scraper with EP tubes to collect. At the end, the liver cells were broken up by ultrasonic instrument, and the supernatant was taken to be measured after centrifugation.

Determination of Triglyceride, Total Cholesterol, High-Density Lipoprotein Cholesterol, and Low-Density Lipoprotein Cholesterol Content

The levels of total cholesterol (TC), triglyceride (TG), high-density lipoprotein cholesterol (HDL-Ch), as well as low-density lipoprotein cholesterol (LDL-Ch) in each group were determined by using commercial kits (Nanjing Jiancheng biology Co., Ltd.) and strictly following the instructions from manufacturer.

Extraction of Total RNA and Primer Designing

The total RNA of the liver cells was extracted by using Trizol agentia (TaKaRa Biotechnology Co., Ltd.) in accordance with the specifications from the manufacturer. The RNA quality and concentration were measured by using a MicroSpectrophotometer as well as 1% agarose gel electrophoresis. Afterwards, the cDNA (complementary DNA) was obtained by means of reverse transcription via a Reverse Transcription reagent Kit (TaKaRa Biotechnology Co., Ltd.).

The reaction of cDNA synthesis (20 μL) was carried out in a system containing 6 μL of RNase-free ddH2O, 1 μL of total RNA, 1 μL of gDNA Eraser, and 2 μL of DNA Eraser Buffer ($5 \times$) and was then incubated at a temperature of 42°C and lasted for 2 min. After that, the system was supplemented with the following reagents: 4 μL of RNase-free ddH2O, 1 μL of RT Primer Mix, 1 μL of Prime Script RT Enzyme Mix I, and 4 μL of Prime Script Buffer 2 ($5\times$). The reaction happened at a temperature of 37°C and for 15 min, then 85°C 5 s and 4°C 10 min. Finally, the cDNA obtained by reverse transcription was conserved in a freezer (-20°C) for the next quantitative PCR. The primer sequences of LKB1, AMPKα1, CPT1, PPARα, ACC, FAS, HMGR, GAPT, and HNF4α were presented in Table 1. The internal reference gene used in the present study is NADPH.

Real-Time Quantitative Polymerase Chain Reaction

The transcription levels of LKB1, AMPKα1, CPT1, PPARα, ACC, FAS, HMGR, GAPT, and HNF4α genes were evaluated via Real-Time Quantitative PCR using the Quant Studio 7 Flex System. The real-time quantitative polymerase chain reaction system included 3 μL of water, 1 μL of cDNA templates, 0.2 μL of $50 \times$ ROX referencing dye, 5 μL of $2 \times$ SYBR Premix Ex Tap II, and 0.4 μL of forward and reverse primers (10 pmol/mL). The real-time quantitative polymerase chain reaction procedure was set as follows: 95°C for 5 min, 40 cycles at 95°C for 15 s, 62°C for 1 min, and extension at 72°C for 60 s. The Quant Studio 7 Flex System was used to perform the all reactions. Then, the melt curve

Table 1. Primer sequences.

| Gene	Accession No.	Products (bp)	Sequences (5′-3′)
AMPKα1	NM_001039603	216	F: 5′-TGTTCCTTCCCCCTTTATTC-3′ R: 5′-GCAACATCTCTCTTGGCACT-3′
LKB1	NM_001045833	214	F: 5′-GGAGATGCTGGACTCTGAAA-3′ R: 5′-CCCACACACACAGTACTCCA-3′
ACC	NM_205505	118	F: 5′-GTCCTGATAGCCAACAATGG-3′ R: 5′-CAGGAGTCACCATGACAACA-3′
FAS	NM_205155	117	F: 5′-AAAGCAATTCGTCACGGACA-3′ R: 5′-GGCACCATCAGGACTAAGCA-3′
CPT1	DQ314726	164	F: 5′-GGCGTTTCGTATATCATTGC-3′ R:5′-GCCTTTATTGCTCATTGCTG-3′
GPAT	EU049888.1	92	F: 5′-TGTGGAAGGGCTTGTATCGT-3′ R: 5′-TTCCAACACGCGATTTCTGG-3′
HMGR	AB109635	244	F: 5′-CTGGGTTTGGTTCTTGTTCA-3′ R: 5′-ATTCGGTCTCTGCTTGTTCA-3′
HNF4α	AY700581.1	155	F: 5′-TGGTGTTCAAGGATGTCTTGCTG-3′ R: 5′-CAAGCAGGCGTATTCATTGTCGT-3′
PPARα	NM_001001464	220	F:5′-ACGGAGTTCCAATCGC-3′ R: 5′-AACCCTTACAACCTTCACAA-3′
GAPDH	NM_204305	141	F: 5′-TGGCATCCAAGGAGTGAGC-3′ R: 5′-GGGGAGACAGAAGGGAACAG-3′
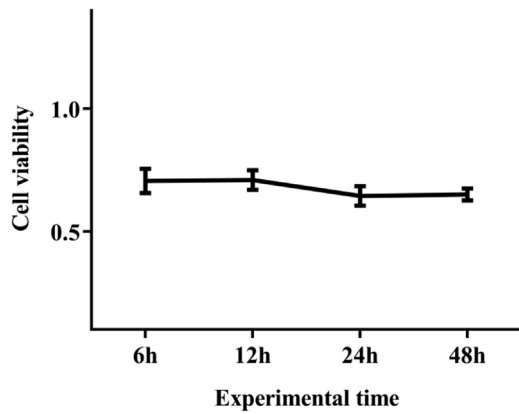
Figure 1. The activity of the liver cells at different times.

of the aforementioned genes was analyzed, and Ct values were acquired for each PCR system. Finally, the means of $2^{-\Delta\Delta Ct}$ were used to calculate and analyze the data.

Statistical Analysis

Softwares of Statistical Package for the Social Sciences (SPSS) version 22.0 (SPSS Inc., Chicago, IL) and Graph Pad Prism 5.01 (Graph Pad Inc., La Jolla, CA) were used for data analysis. All data were analyzed by one-way ANOVA, and the results were showed as mean $\pm$ SD. $P < 0.05$ was conceived as statistically significant. $P < 0.05$ denotes significant difference, and $P < 0.01$ denotes extremely significant difference. Moreover, $*P < 0.05$ and $**P < 0.01$ represent compared with the NH group. $\#P < 0.05$ and $\#\#P < 0.01$ express compared with the SH group.

RESULTS

Identification of Cell Survival Rate and Cell Activity

The cell survival rate confirmed by Trypan Blue staining reached 90%, and a stable culture system was established. The liver cells shown under the inverted microscope were round, with few impurities and dead cells.

After measuring the cell survival rate, we measured the cell activity of hepatocytes by the CCK8 method. The measurement results of hepatocyte activity are showed in Figure 1. There was no significant difference for CCK8 value in each time period. The results suggested that the liver cells have always maintained high activity during the experiment, and there was no significant difference in cell activity at different times.

The Optimum Working Time of AICAR and Compound C in Primary Liver Cells

To determine the best moment for the activator AICAR and inhibitor compound C to work, AMPK activity of hepatocytes was measured with a commercial
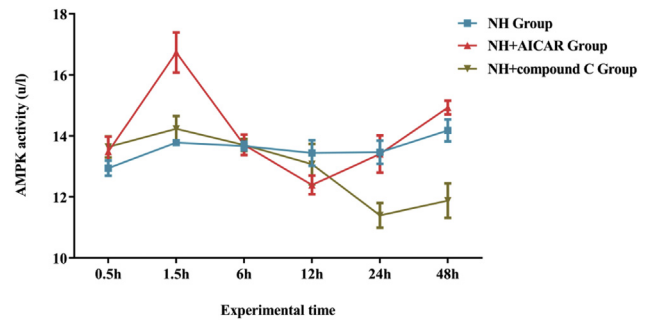

Figure 2. The AMPK activity curve in the liver cells in different groups. Abbreviations: AMPK, AMP-activated protein kinase; NH, normal hepatocytes.

kit (Nanjing Jiancheng Biological Engineering Co., Ltd., Nanjing 210000, China). The changing curve of AMPK activity in liver cells is showed in Figure 2. In the current experiment, the results indicated that activator AICAR can activate AMPK, and under the action of AICAR, the AMPK activity of hepatocytes reached the highest at 1.5 h. Moreover, the inhibitor compound C can inhibit AMPK, and the AMPK activity of liver cells decreased to the lowest at 24 h under the action of compound C.

Results of Identification of Oil Red O Staining in the Liver Cells

The results of oil red O staining are showed in Figure 3. Oil red O staining turned the lipid droplets around the nucleus red, while the nucleus appears blue. Compared with the NH group, at 1.5 h, the increase of lipid droplets in the SH group was not obvious; at 6 h, red stained lipid droplets around the nucleus increased observably in the SH group; at 12 h, the particles of lipid droplets began to gather into small bubbles in the SH group; at 24 h, the confluence area of lipid droplets increased significantly, reaching the highest degree of convergence in the SH group. There is no significant change in lipid droplets in the NH group. The results showed that the liver cells in the SH group had produced fatty degeneration, and the degree gradually increased over time.

Results of Quantitative Identification of Oil Red O Staining in the Liver Cells

Quantitative results of oil red O staining are showed in Figure 4. At 6 h, compared with the NH group, the content of lipid droplet in the hepatocytes rose markedly in the SH group ($P < 0.05$), at 12 h and 24 h, compared with the NH group, and the lipid droplet content of the hepatocytes increased extremely markedly in the SH group ($P < 0.01$). The results further prove that the model of SH was successfully established.

Results of Determination of TG, TC, HDL-Ch and LDL-Ch Content in the Liver Cells

Well known, TG, TC, LDL-Ch, and HDL-Ch are the representative indicators for studying lipid metabolism.
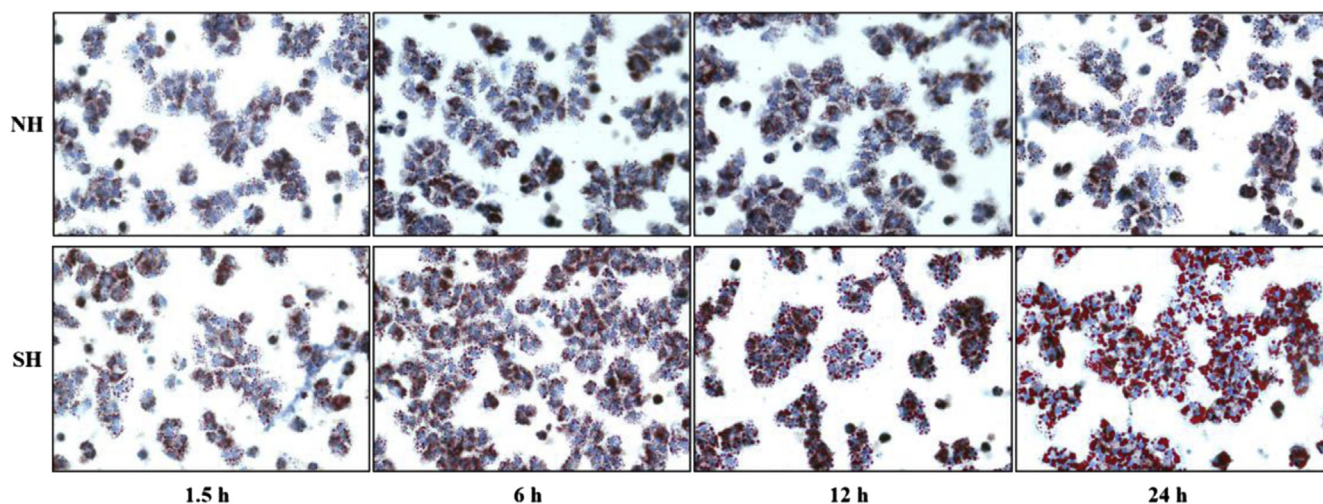
Figure 3. Results of identification of oil red O staining for the liver cells at different times. Abbreviations: NH, normal hepatocytes group; SH, steatosis hepatocytes group.

We thus determined the content of TG, TC, LDL-Ch, and HDL-Ch in the hepatocytes. As shown in Figure 5, at 1.5 h and 24 h, compared with the NH group, the concentration of TG, TC, and LDL-Ch in the SH group increased obviously, while the content of HDL-Ch in the SH group decreased markedly. Conversely, the TG, TC, and LDL-Ch concentration in the SH + AICAR group was significantly lower than those in the SH group, while the content of HDL-Ch in the SH + AICAR group increased significantly (24 h).

These results indicate that AMPK activation significantly decreased the lipid content in the layer hepatocytes. However, compound C treatment inhibited the aforementioned effect of AMPK.

Results of Determination of mRNA Expression Levels of LKB1 and AMPKα1 in Liver Cells

AMPK, the sensor of cellular energy status and the metabolic master switch, plays a significant role in lipid metabolism by regulating the key transcription factors involved in lipid oxidation and lipid synthesis. Furthermore, as the upstream kinase of AMPK, LKB1 (liver kinase B1) is involved in the activation of AMPK. Therefore, we detected the mRNA levels of LKB1 and AMPKα1. As shown in Figures 6A, 6B, at 1.5 h and 24 h, compared with the NH group, the mRNA levels of LKB1 and AMPKα1 decreased significantly in the SH group. However, the LKB1 and AMPKα1 mRNA levels increased markedly in the SH + AICAR group compared with those in the SH group. Moreover, compound C treatment significantly decreased the AMPK mRNA expression (24 h). These results suggest that steatosis may inhibit the mRNA expression of LKB1 and AMPK in layer hepatocytes, thereby inhibiting the AMPK signaling pathway.

Results of Determination of mRNA Expression Levels of FA Oxidation and Lipid Synthesis Related Genes in Liver Cells

To further elucidate the relationship between AMPK signaling pathway and lipid metabolism in liver cells, the mRNA expression levels of lipid metabolism-related genes were determined. Peroxisome proliferator-activated receptor α (PPARα) and carnitine palmitoyl transferase-1 (CPT1) are the key genes involved in lipid oxidation of liver cells. As shown in Figures 6C, 6D, at 1.5 h and 24 h, compared with the NH group, the mRNA expression of CPT1 decreased significantly in the SH group. Conversely, CPT1 mRNA level was significantly enhanced in the SH + AICAR group compared with that in the SH group. Interestingly, the mRNA expression level of PPARα was significantly higher in the SH group than that in the NH group, and after
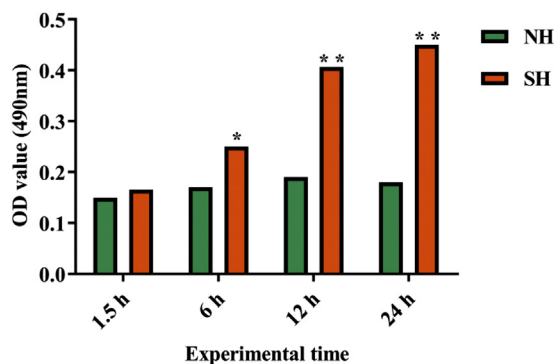

Figure 4. Results of quantitative identification of oil red O staining in the hepatocytes. The data in the figure mean ± SD. $*P < 0.05$ represents significant difference between the NH group and the SH group. $**P < 0.01$ represents extremely significant difference between the NH group and the SH group. $P < 0.05$ is conceived as statistically significant. The method of T test is used to compute the statistical difference. Abbreviations: NH, normal hepatocytes group; SH, steatosis hepatocytes group.
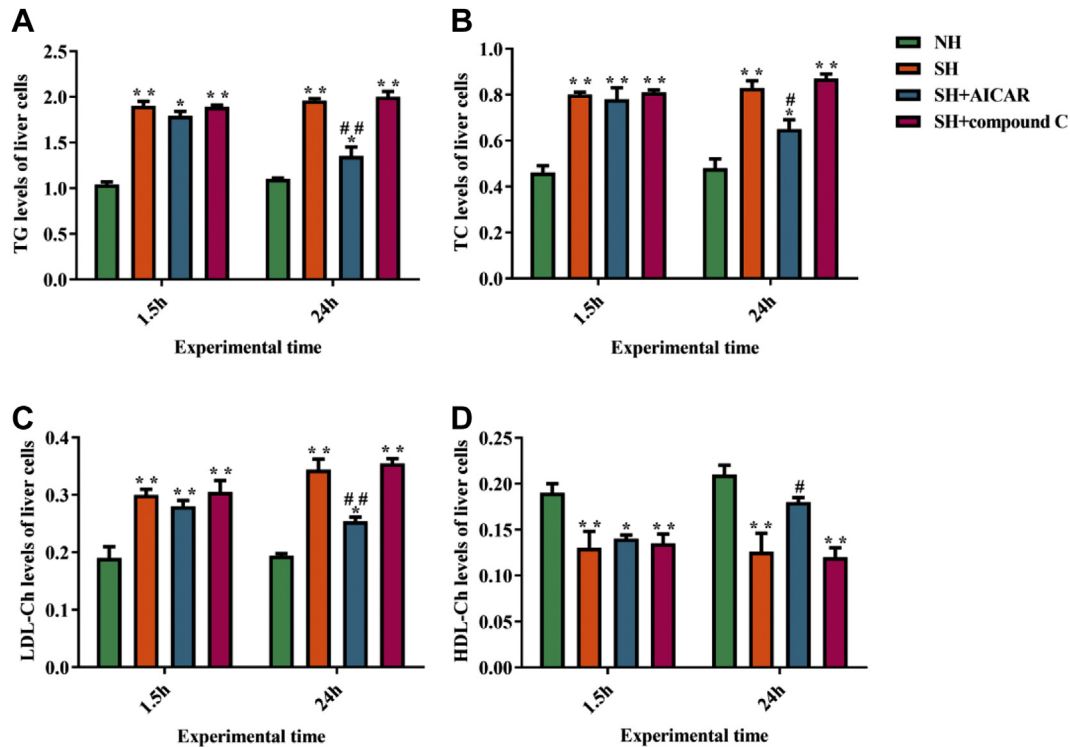
Figure 5. Results of determination of (A) TG, (B) TC, (C) HDL-Ch, and (D) LDL-Ch content in the liver cells. The data in the figure mean ± SD. *$P < 0.05$, **$P < 0.01$ denote compared with the NH group. #$P < 0.05$, ##$P < 0.01$ denote compared with the SH group. $P < 0.05$ is conceived as statistically significant. The one-way analysis of variance (ANOVA) is used to compute the statistical difference. Abbreviations: HDL-Ch, high-density lipoprotein cholesterol; LDL-Ch, low-density lipoprotein cholesterol; NH, normal hepatocytes group; SH, steatosis hepatocytes group; TC, total cholesterol; TG, triglyceride.

activation of AMPK by AICAR, PPARα mRNA level was significantly enhanced (1.5 h). Collectively, these results indicate that AMPK may ameliorate steatosis by increasing FA oxidation in layer hepatocytes.

3-hydroxy-3-methyl glutaryl coenzyme A reductase (HMGR), Sn-glycerol-3-phosphate acyltransferase (GPAT), fatty acid synthase (FAS), acetyl CoA carboxylase (ACC), and hepatocyte nuclear factor 4 (HNF4α) are the key genes involved in lipid synthesis of liver cells. As shown in Figures 6E–I, in the SH group, the mRNA levels of HMGR, GPAT, FAS, ACC, and HNF4α genes enhanced markedly compared with those in the NH group (1.5 h and 24 h). Conversely, compared with the SH group, the mRNA levels of HMGR, GPAT, FAS, ACC, and HNF4α declined obviously in the SH + AICAR group (1.5 h and 24 h). Overall, these results indicate that AMPK may ameliorate fatty degeneration by decreasing lipid synthesis in laying hens. Synthesizing the aforementioned information, the experimental results are plotted into a signal path diagram (Figure 7).

DISCUSSION

FLHS is a type of metabolic disease and is also a chronic hepatic disease, which contains a series of liver pathological changes such as simplex steatosis, nonalcoholic steatohepatitis, liver fibrosis, and even cirrhosis (McCullough, 2004; Cheng et al., 2018). FLHS usually occurs in caged laying hens, and it is featured by the excessive accumulation of triglycerides in the cytoplasm of hepatocytes. Importantly, AMPK is a crucial energy sensor as well as metabolic master switch, which is responsible for regulating the homeostasis of lipid metabolism in liver cells (Hardie, 2015). AMPK is activated under stress conditions such as exercise, hunger, ischemia, and shock. Unfortunately, up to now, the specific relationship between AMPK signaling pathway and lipid metabolism in layer liver cells is still unclear. Our study suggested that steatosis inhibits AMPK activity, while activated AMPK signaling pathway enhances FA oxidation and reduces lipid synthesis, thereby inhibiting steatosis in hepatocytes of laying hen. These results may be helpful to the treatment and prevention of FLHS and further research on hepatocyte lipid metabolism.

Exogenous addition of excess FA is often used to establish *in vitro* models of cell steatosis that reliably reproduce key features of liver steatosis. In Lin's research on lipid metabolism, HepG 2 cells were exposed to a FA overload environment to study the lipid-lowering effect of AMPK activation induced by theaflavins (Lin et al., 2007). Moreover, in the previous study, oleic acid and palmitic acid were used in combination to induce cell steatosis. Similarly, in the present study, the model of SH was successfully established with oleic acid and palmitic acid according to the previous study (Gomez-Lechon et al., 2007), which was confirmed by Oil Red O staining as well as Oil Red O quantification. Compared with the single oleic acid–induced steatosis in hepatocytes of laying hens, this combined induction
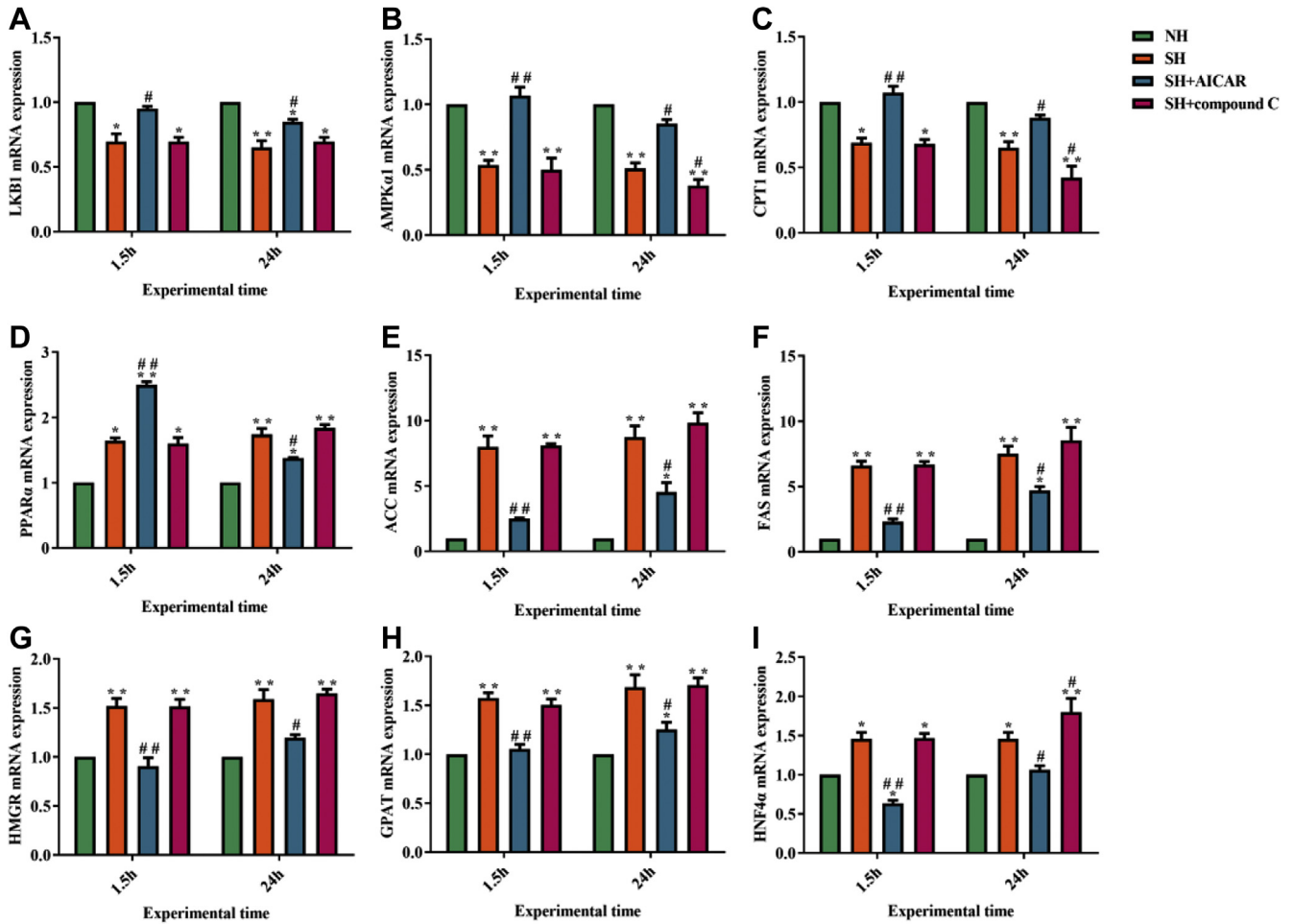
Figure 6. Results of determination of mRNA expression levels of AMPK signaling pathway-related genes including (A) liver kinase B1 (LKB1), (B) AMP-activated protein kinase α1 (AMPKα1), (C) carnitine palmitoyl transferase-1 (CPT1), (D) peroxisome proliferator-activated receptor (PPARα), (E) acetyl CoA carboxylase (ACC), (F) fatty acid synthase (FAS), (G) 3-hydroxy-3-methyl glutaryl coenzyme A reductase (HMGR), (H) Sn-glycerol-3-phosphate acyltransferase (GPAT), (I) hepatocyte nuclear factor 4 (HNF4α) in the liver cells. The data in the figure mean ± SD. *$P < 0.05$ and **$P < 0.01$ denote compared with the NH group. #$P < 0.05$ and ##$P < 0.01$ denote compared with the SH group. $P < 0.05$ is conceived as statistically significant. The one-way analysis of variance (ANOVA) is used to compute the statistical difference.

method is more effective. As a matter of fact, before the formal experiment, the FA gradient concentration was set to determine the optimal induced concentration. During the induction period, punctate lipid droplets appeared in the cytoplasm of liver cells of laying hens, and the small lipid droplets would converge into larger lipid droplets with increasing induction time. Oil Red O is a fat-soluble dye, which is highly soluble in fat, and it can specifically color neutral fats such as triglycerides in tissues. Liver cells take in FA and esterify them into stored neutral lipid droplets. Therefore, the formation of lipid droplets in SH can be visually observed by using Oil Red O staining method (Wu et al., 2019). In addition, the establishment of simplex SH model was evaluated jointly by Oil Red O staining combined with Oil Red O quantification.

AICAR is considered to be a specific activator of AMPK and has been confirmed by many research experiments. In mechanism, AICAR is rapidly processed into 5-aminoimidazole-4-carboxamide ribonucleotide

(**ZMP**) by adenylase. ZMP is an analog of AMP, which can mimic the biological effects of AMP, that is, activate AMPK. Thus, AICAR is widely used to study the activated AMPK signaling pathway in many *in vivo* and *in vitro* experiments (Sullivan et al., 1994; Guigas et al., 2009). Besides, in previous research, a small-molecule AMPK inhibitor compound C was discovered and identified by Zhou (Zhou et al., 2001) and was extensively used in various studies as a AMPK inhibitor. The biochemical and cellular effects of compound C are attributed to its role of AMPK inhibition. In the present study, AMPK activator AICAR and inhibitor compound C have been used to activate and inhibit the AMPK signaling pathway, respectively. Furthermore, to determine the optimal activation and inhibition time, we measured the activity of AMPK at different time periods. Under present culture condition, AICAR has the largest effect of activation at 1.5 h, and compound has the most obvious inhibition effect at 24 h.
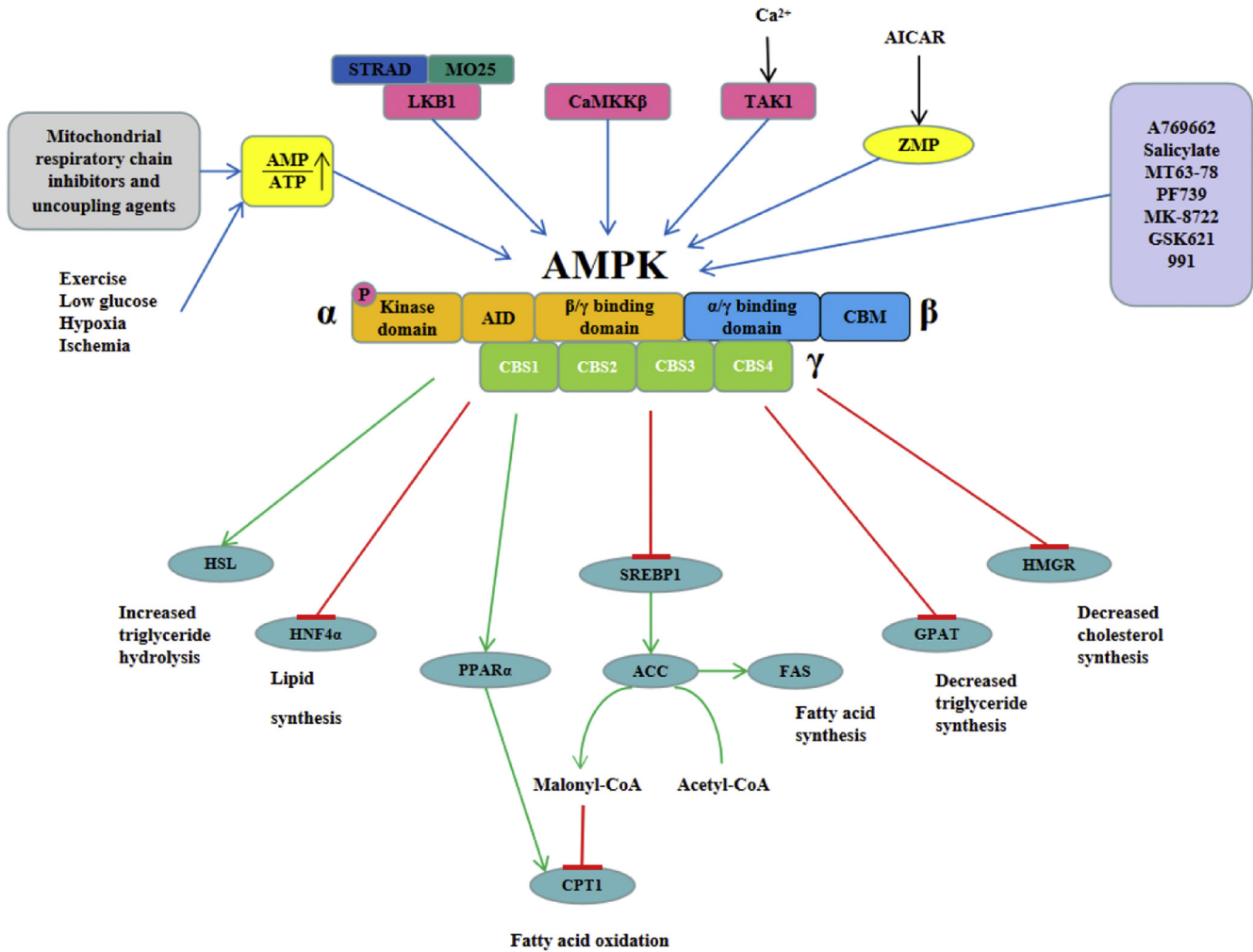
Figure 7. Relationship between AMPK signaling pathway and lipid metabolism in laying hen hepatocytes. The figure shows the ways and methods of activating the AMPK signaling pathway (indicated by the blue arrows). Activated AMPK may ameliorate hepatocytes steatosis by upregulating the mRNA levels of fatty acid oxidation–related genes such as CPT1 and PPARα and downregulating the mRNA levels of lipid synthesis-related genes such as SREBP1, ACC, FAS, HMGR, GPAT, and HNF4α (green arrows indicate promotion, red lines represent inhibition).

As we know, TG, TC, HDL-Ch, and LDL-Ch are representative indicators for studying lipid metabolism. Previous research has showed that when the liver has undergone steatosis, the levels of TG and TC in the liver were significantly increased (Gao et al., 2019). Moreover, a study from Yamazaki et al. shows that the mice suffering from fatty liver were featured by increased levels of TC and TG in the hepatocytes (Yamazaki et al., 2008). Similar to these results, in the present study, compared with the NH group, the content of TC and TG in the SH group increased significantly. Generally speaking, the fatty degeneration of liver is characterized by aggregation of TG in the cytoplasm of hepatocytes. In this study, obvious fat vacuoles were observed in the steatosis hepatocyte model. This suggested the undue accumulation of TG in the hepatocytes. Simultaneously, it also showed that we successfully modeled the liver cells of laying hens *in vitro*. According to Griffin's research, hepatic lipid metabolism was mainly accomplished via the synthesis and decomposition of FA and the production and output of fats (Griffin et al., 1992). While the transport of lipid

is mainly achieved by HDL-Ch and LDL-Ch; hence, HDL-Ch and LDL-Ch play an important role in lipid metabolism. In the present study, compared with the NH group, the content of LDL-Ch augmented obviously in the SH group. Similar to our results, the study of Gao showed that LDL-Ch content rose in the fatty liver group and was much higher than that in the control group (Gao et al., 2019). This may be because LDL-Ch is responsible for the lipid output in the liver. Thus, with the increase of TG in hepatocytes, the content of LDL-Ch is also enhanced. On the contrary, HDL-Ch is responsible for transporting cholesterol back to the liver, so when the excessive lipid accumulates in the liver, the effect of HDL-Ch declines and the content decreases.

AMPK, the sensor of cellular energy status and the metabolic master switch, is activated by an increase in the AMP/ATP ratio (Saha and Ruderman, 2003), and recovering the energy balance through facilitating the energy generation pathways such as lipolysis and FA oxidation, as well as restraining ATP-consuming pathways, such as FA synthesis, cholesterol synthesis, and triglyceride synthesis. In this study, compared with the

normal group, the mRNA level of AMPKα1 gene decreased markedly in the steatosis group. So, the current results showed that the decline of AMPK mRNA level in the hepatocytes is closely related to the steatosis of the liver. In addition, research has indicated that high fat exposure observably reduced the expression of AMPK (Liu et al., 2006), which is similar to our situation. Conversely, the overexpression of AMPK in the liver could decrease the content of triglyceride, hepatic steatosis, as well as the expression of lipogenic gene (Seo et al., 2009), which showed the antagonism between AMPK activation and lipogenesis. Besides, after adding activator AICAR to SH group, the mRNA expression of AMPKα1 was obviously improved compared with SH group without AICAR.

LKB1, the upstream kinase of AMPK, is involved in the activation of AMPK (Sundararaman et al., 2016). It is well known that AMPK is activated by the phosphorylation of Thr-172 catalyzed by LKB1 within the α subunit (Shaw et al., 2005), and LKB1 mediates AMPK activation under the circumstance of energy stress. In our study, the mRNA level of LKB1 declined significantly in the SH group compared with the NH group. Conversely, LKB1 mRNA expression was markedly enhanced in the SH + AICAR group. It indicated that the mRNA level of LKB1 is closely associated with the activity of AMPK. In the liver, the activation of AMPK leads to the inactivation of ACC; furthermore, as the key regulator of FAS generation, the content of FAS is positively correlated with ACC activity (Lin and Hardie, 2018). As a result, AMPK activation inhibits the synthesis of FA. In addition, activation of AMPK downregulates the expression of SREBP-1c (Li et al., 2014), while SREBP-1c is the critical factor of TG synthesis (Li et al., 2011). Thus, stimulation of AMPK activation, thereby inhibiting the activity of SREBP-1c, ACC, and FAS, can reduce accumulation of TG and FA in the liver. Besides, other studies have showed that AMPK activation inhibits the expression of ACC and FAS through downregulating SREBP-1c (Zhou et al., 2001). In the current research, the mRNA levels of FAS and ACC in the SH + AICAR group were significantly reduced compared with those in the SH group. However, in the SH group, AMPK mRNA level was remarkably downregulated, while the mRNA levels of ACC and FAS increased significantly. Similarly, in the previous studies (Kohjima et al., 2007), the mRNA expression of ACC and FAS was proved to be upregulated in the liver of nonalcoholic fatty liver disease.

The study of Nguyen suggested that activation of AMPK can inhibit GPAT activity and synthesis of triacylglycerol (Nguyen et al., 2008). Moreover, Muoio et al. found the activity of GPAT decreased after addition of AICAR to the hepatocytes cultured *in vitro*, testifying that the activity of GPAT is negatively correlated with AMPK activity (Muoio et al., 1999). In our study, compared with SH group, the mRNA expression level of GPAT reduced obviously in the SH + AICAR group, indicating that activation of AMPK may suppress the synthesis of triglyceride. This is the same result as Muoio. In contrast, compared to the NH group, the mRNA level of GPAT increased significantly in the SH group. HMGR is the rate-limiting enzyme in cholesterol anabolism. The study from Carling et al. has indicated that activation of AMPK can suppress the expression of HMGR (Carling et al., 1987). In addition, after the addition of AICAR in the suspension cultured rat liver cells, the activity of HMGR was observably decreased compared with that in the control group (Corton et al., 1995). In this research, in the SH + AICAR group, HMGR mRNA level decreased significantly compared with that in the SH group, indicating that excitation of AMPK inhibited the synthesis of cholesterol. As the downstream factor of AMPK, HNF4α is the key factor of liver lipid synthesis (Song et al., 2013). The research by Gao et al. showed that the mRNA level of HNF4α is significantly increased in the liver of chickens with fatty liver (Gao et al., 2019). Meanwhile, Hong et al. showed that the expression of HNF4α declined after AMPK activation (Hong et al., 2003). Our results of study are same as them.

CPT1 is the key enzyme regulating FA oxidation, which exerts a significant role in the β-oxidation of long-chain FA. A study found that AMPK regulates FA oxidation through AMPK-ACC-malonic acid monoacyl coenzyme A-CPT1 mechanism (Jensen et al., 2009). After AMPK activation, the activity of ACC is inhibited, thereby reducing the activity of malonic acid monoacyl-CoA, and consequently, the allosteric inhibition of CPT1 caused by malonic acid monoacyl-CoA is alleviated. So, the β-oxidation of FA is facilitated. In the present study, the mRNA expression of CPT1 was observably enhanced in the SH + AICAR group compared with that in the SH group. Thus, it can be seen, activation of AMPK inhibited ACC activity, thereby suppressing the activity of malonic acid monoacyl-CoA and decreasing the allosteric inhibition of CPT1. So, the mRNA level of CPT1 was significantly increased after adding AICAR to the SH group. Conversely, the CPT1 mRNA level was markedly decreased in the SH group. All the aforementioned results explain that CPT1 activity is consistent with AMPK activity. PPAR is a ligand-activated receptor in the nuclear hormone receptor family. After PPAR is activated by a ligand, it forms a heterodimer with the retinoid X receptor, and the heterodimer binds to the PPAR reaction element in the target gene promoter upstream, ultimately regulating transcription of target genes. Furthermore, PPARα exerts a significant function on FA oxidation and reducing lipid level. Free FA are natural ligands of PPARα. When FA concentration rises, they will enter cells and activate PPARα to start FA oxidation pathway (Konstandi et al., 2013). In addition, many studies have showed that AMPK can ameliorate lipid metabolism through the AMPK/PPARα/CPT1 pathway (Bordoloi et al., 2019). In line with the aforementioned results, in our experiment, after AMPK activation, the mRNA expression of PPARα and CPT1 were remarkably improved. Interestingly,

the mRNA level of PPARα also rose in the SH group compared with that in the NH group. This may be because PPARα is responsible for the oxidation of FA. In the steatosis liver cells, the intracellular lipid content increased, so the expression of PPARα was also enhanced. In the study of Gao et al. (Gao et al., 2019), the mRNA expression level of PPARα increased significantly in the liver of laying hens with fatty liver. Obviously, this is also similar to our results.

In conclusion, our results suggest that AMPK signaling pathway is involved in the process of hepatocytes steatosis in laying hens, and steatosis could significantly decline LKB1 and AMPK mRNA levels. However, with the activation of AMPK, the mRNA expression levels of lipid synthesis-related genes such as HMGR, GPAT, FAS, ACC, and HNF4α are reduced, thereby decreasing the lipid production in liver cells. Furthermore, with the increase of AMPK activity, the mRNA levels of lipid oxidation-related genes such as CPT1 and PPARα are also enhanced, thereby increasing the lipid oxidation of hepatocytes. As a result, the lipid in layer liver cells is reduced, and the steatosis is suppressed or ameliorated. To sum up, our study may partially clarify the regulation mechanism of AMPK signaling pathway on lipid metabolism in laying hen hepatocytes and also laid the foundation for further research on FLHS.

ACKNOWLEDGMENTS

DISCLOSURES

The authors declare no conflict of interest.

SUPPLEMENTARY DATA

Supplementary data associated with this article can be found in the online version at https://doi.org/10.1016/j.psj.2020.10.059.

REFERENCES

Bordoloi, J., D. Ozah, T. Bora, J. Kalita, and P. Manna. 2019. Gamma-glutamyl carboxylated Gas6 mediates the beneficial effect of vitamin K on lowering hyperlipidemia via regulating the AMPK/SREBP1/PPARalpha signaling cascade of lipid metabolism. J. Nutr. Biochem. 70:174–184.

Boudaba, N., A. Marion, C. Huet, R. Pierre, B. Viollet, and M. Foretz. 2018. AMPK re-activation suppresses hepatic steatosis but its downregulation does not promote fatty liver development. Ebiomedicine 28:194–209.

Carling, D., V. A. Zammit, and D. G. Hardie. 1987. A common bicyclic protein kinase cascade inactivates the regulatory enzymes of fatty acid and cholesterol biosynthesis. FEBS Lett. 223:217–222.

Cheng, S., S. Liang, Q. Liu, Z. Deng, Y. Zhang, J. Du, Y. Zhang, S. Li, B. Cheng, and C. Ling. 2018. Diosgenin prevents high-fat diet-induced rat non-alcoholic fatty liver disease through the AMPK and LXR signaling pathways. Int. J. Mol. Med. 41:1089–1095.

Corton, J. M., J. G. Gillespie, S. A. Hawley, and D. G. Hardie. 1995. 5-aminoimidazole-4-carboxamide ribonucleoside. A specific method for activating AMP-activated protein kinase in intact cells? Eur. J. Biochem. 229:558–565.

Gao, X., P. Liu, C. Wu, T. Wang, G. Liu, H. Cao, C. Zhang, G. Hu, and X. Guo. 2019. Effects of fatty liver hemorrhagic syndrome on the AMP-activated protein kinase signaling pathway in laying hens. Poult. Sci. 98:2201–2210.

Gomez-Lechon, M. J., M. T. Donato, A. Martinez-Romero, N. Jimenez, J. V. Castell, and J. E. O'Connor. 2007. A human hepatocellular in vitro model to investigate steatosis. Chem. Biol. Interact. 165:106–116.

Griffin, H. D., K. Guo, D. Windsor, and S. C. Butterwith. 1992. Adipose tissue lipogenesis and fat deposition in leaner broiler chickens. J. Nutr. 122:363–368.

Guigas, B., K. Sakamoto, N. Taleux, S. M. Reyna, N. Musi, B. Viollet, and L. Hue. 2009. Beyond AICA riboside: in search of new specific AMP-activated protein kinase activators. IUBMB Life 61:18–26.

Hardie, D. G. 2015. AMPK: positive and negative regulation, and its role in whole-body energy homeostasis. Curr. Opin. Cell Biol. 33:1–7.

Hong, Y. H., U. S. Varanasi, W. Yang, and T. Leff. 2003. AMP-activated protein kinase regulates HNF4alpha transcriptional activity by inhibiting dimer formation and decreasing protein stability. J. Biol. Chem. 278:27495–27501.

Jensen, T. E., J. F. Wojtaszewski, and E. A. Richter. 2009. AMP-activated protein kinase in contraction regulation of skeletal muscle metabolism: necessary and/or sufficient? Acta Physiol. (Oxf.) 196:155–174.

Kohjima, M., M. Enjoji, N. Higuchi, M. Kato, K. Kotoh, T. Yoshimoto, T. Fujino, M. Yada, R. Yada, N. Harada, R. Takayanagi, and M. Nakamuta. 2007. Re-evaluation of fatty acid metabolism-related gene expression in nonalcoholic fatty liver disease. Int. J. Mol. Med. 20:351–358.

Konstandi, M., Y. M. Shah, T. Matsubara, and F. J. Gonzalez. 2013. Role of PPARalpha and HNF4alpha in stress-mediated alterations in lipid homeostasis. PLoS One 8:e70675.

Li, Y., H. Ding, J. Dong, R. S. Ur, S. Feng, X. Wang, J. Wu, Z. Wang, G. Liu, X. Li, and X. Li. 2019. Glucagon attenuates lipid accumulation in cow hepatocytes through AMPK signaling pathway activation. J. Cell Physiol. 234:6054–6066.

Li, H., Q. Min, C. Ouyang, J. Lee, C. He, M. H. Zou, and Z. Xie. 2014. AMPK activation prevents excess nutrient-induced hepatic lipid accumulation by inhibiting mTORC1 signaling and endoplasmic reticulum stress response. Biochim. Biophys. Acta 1842:1844–1854.

Li, Y., S. Xu, M. M. Mihaylova, B. Zheng, X. Hou, B. Jiang, O. Park, Z. Luo, E. Lefai, J. Y. Shyy, B. Gao, M. Wierzbicki, T. J. Verbeuren, R. J. Shaw, R. A. Cohen, and M. Zang. 2011. AMPK phosphorylates and inhibits SREBP activity to attenuate hepatic steatosis and atherosclerosis in diet-induced insulin-resistant mice. Cell Metab. 13:376–388.

Lin, S. C., and D. G. Hardie. 2018. AMPK: sensing glucose as well as cellular energy status. Cell Metab. 27:299–313.

Lin, C. L., H. C. Huang, and J. K. Lin. 2007. Theaflavins attenuate hepatic lipid accumulation through activating AMPK in human HepG2 cells. J. Lipid Res. 48:2334–2343.

Liu, Y., Q. Wan, Q. Guan, L. Gao, and J. Zhao. 2006. High-fat diet feeding impairs both the expression and activity of AMPKa in rats' skeletal muscle. Biochem. Biophys. Res. Commun. 339:701–707.

McCullough, A. J. 2004. The clinical features, diagnosis and natural history of nonalcoholic fatty liver disease. Clin. Liver Dis. 8:521–533.

Mete, A., F. Giannitti, B. Barr, L. Woods, and M. Anderson. 2013. Causes of mortality in backyard chickens in northern California: 2007-2011. Avian Dis. 57:311–315.

Muoio, D. M., K. Seefeld, L. A. Witters, and R. A. Coleman. 1999. AMP-activated kinase reciprocally regulates triacylglycerol

synthesis and fatty acid oxidation in liver and muscle: evidence that sn-glycerol-3-phosphate acyltransferase is a novel target. Biochem. J. 338(Pt 3):783–791.

Muse, E. D., S. Obici, S. Bhanot, B. P. Monia, R. A. McKay, M. W. Rajala, P. E. Scherer, and L. Rossetti. 2004. Role of resistin in diet-induced hepatic insulin resistance. J. Clin. Invest. 114:232–239.

Nguyen, P., V. Leray, M. Diez, S. Serisier, J. Le Bloc'H, B. Siliart, and H. Dumon. 2008. Liver lipid metabolism. J. Anim. Physiol. Anim. Nutr. (Berl.) 92:272–283.

Rozenboim, I., J. Mahato, N. A. Cohen, and O. Tirosh. 2016. Low protein and high-energy diet: a possible natural cause of fatty liver hemorrhagic syndrome in caged White Leghorn laying hens. Poult. Sci. 95:612–621.

Ruderman, N. B., D. Carling, M. Prentki, and J. M. Cacicedo. 2013. AMPK, insulin resistance, and the metabolic syndrome. J. Clin. Invest. 123:2764–2772.

Saha, A. K., and N. B. Ruderman. 2003. Malonyl-CoA and AMP-activated protein kinase: an expanding partnership. Mol. Cell Biochem. 253:65–70.

Seo, E., E. J. Park, Y. Joe, S. Kang, M. S. Kim, S. H. Hong, M. K. Park, D. K. Kim, H. Koh, and H. J. Lee. 2009. Overexpression of AMPKalpha1 ameliorates fatty liver in Hyperlipidemic diabetic rats. Korean J. Physiol. Pharmacol. 13:449–454.

Shaw, R. J., K. A. Lamia, D. Vasquez, S. H. Koo, N. Bardeesy, R. A. Depinho, M. Montminy, and L. C. Cantley. 2005. The kinase LKB1 mediates glucose homeostasis in liver and therapeutic effects of metformin. Science 310:1642–1646.

Song, C. Y., J. Shi, X. Zeng, Y. Zhang, W. F. Xie, and Y. X. Chen. 2013. Sophocarpine alleviates hepatocyte steatosis through activating AMPK signaling pathway. Toxicol. In Vitro 27:1065–1071.

Sullivan, J. E., K. J. Brocklehurst, A. E. Marley, F. Carey, D. Carling, and R. K. Beri. 1994. Inhibition of lipolysis and lipogenesis in isolated rat adipocytes with AICAR, a cell-permeable activator of AMP-activated protein kinase. FEBS Lett. 353:33–36.

Sundararaman, A., U. Amirtham, and A. Rangarajan. 2016. Calcium-oxidant signaling network regulates AMP-activated protein kinase (AMPK) activation upon matrix deprivation. J. Biol. Chem. 291:14410–14429.

Winder, W. W., and D. G. Hardie. 1999. AMP-activated protein kinase, a metabolic master switch: possible roles in type 2 diabetes. Am. J. Physiol. 277:E1–E10.

Wu, L., Y. Wang, G. Chi, B. Shen, Y. Tian, Z. Li, L. Han, Q. Zhang, and H. Feng. 2019. Morin reduces inflammatory responses and alleviates lipid accumulation in hepatocytes. J. Cell Physiol. 234:19785–19798.

Yamazaki, Y., S. Kakizaki, D. Takizawa, T. Ichikawa, K. Sato, H. Takagi, and M. Mori. 2008. Interstrain differences in susceptibility to non-alcoholic steatohepatitis. J. Gastroenterol. Hepatol. 23:276–282.

Zhou, G., R. Myers, Y. Li, Y. Chen, X. Shen, J. Fenyk-Melody, M. Wu, J. Ventre, T. Doebber, N. Fujii, N. Musi, M. F. Hirshman, L. J. Goodyear, and D. E. Moller. 2001. Role of AMP-activated protein kinase in mechanism of metformin action. J. Clin. Invest. 108:1167–1174.